Journal of Structural Engineering Vol.42A(March 1996) JSCE

INFLUENCE OF LOCAL IMPERFECTIONS ON BUCKLING STRENGTH OF RETICULATED SHELLS

Shiro KATO* and Itaru MUTOH**

*Dr. of Eng., Professor, Dept. of Architecture & Civil Engineering, Toyohashi University of Technology, Toyohashi 441

**Assoc. Prof., Dept. of Architecture & Civil Engineering, Gifu National College of Technology, Gifu 501-04

This paper presents several investigations into: how an imperfection should be characterized in the design stage and the effects of various types of shape imperfections would appear in the reduction of the buckling strength of large-spanned reticulated shells or space frames. An attempt is made to evaluate the reduction in collapse load due to the imperfection specified by both inward-dimple shape with diameter of buckling half wavelength of equivalent continuum shell and magnitude as a fraction of member length. It is noticed that a treatment of geometric imperfection on surface of reticulated shell refered with studies and codes of spherical shells affect to the reduction of elastic buckling loads as well as elasto-plastic buckling loads. However there exists various degree of reductions due to a fundamental structural behaviours depending on characteristic shape parameters and member slenderness ratio. Finally, strength evaluations considering characteristic reduction for reticulated shell domes are discussed by using several strength design curves as a function of the generalized slenderness.

Key Words:*Buckling collapse, Nonlinear analysis, Geometric imperfection, Space frame*

1. Introduction

Reticulated shells in large-spanned configuration with rigid joints, called space frames, have to be evaluated the collapse strength of both elastic and elasto-plastic ranges. However the problems that have to be resolved in the design stage as well as in the application of exact nonlinear numerical analysis to as-built structures, still remain. Amongst many influential factors on the collapse strength of reticulated shells, the effects of initial imperfections on elastic instability and of inelastic behaviour of constituent elements on overall strength dominate the capacity reduction[1].

This study aims to discuss the treatment of initial shape imperfections in a similar way of design guidelines for continuum shells[2)3)4)5)] and of investigations into the characteristic influence on the buckling strength reductions in elastic and elasto-plastic ranges[2)3)]. By carring out several numerical analyses following investigations are presented. How does the measure for imperfection amplitudes in relation to the local sizes, member length, thickness and arc length, as well as to the overall shape parameters, span length, rise and radius of curverture, raise the imperfection sensitivity? Is the degree of reduction of buckling capacity comparable to that for continuum spherical shells, or not? Does the strength curve appear in a similar manner of shells with severe imperfection sensitivity?

2. Review for Treatment of Geometric Imperfections

2.1 Analtytical treatment

Computational studies in both continuum shells and reticulated shells on the imperfection sensitivity have been carried out by exploiting the shape imperfections as one of the bifurcation buckling modes, when shells bifurcated[1)2)3)9)10)]. Also from the elastic or elasto-plastic buckling analysis applied to perfect geometry, some kind of deformation shapes have been used as representative imperfection forms. Otherwise the form of one of linear elastic bending deformations has been often assumed. Furthermore on the basis

of random nature of initial imperfection in as-built structures the stochastic imperfection field has been employed in a way of both fully random variable distributions in spatial and magnitude[11], and bifurcation mode-specific shapes with random amplitudes[12].

2.2 Treatment in design codes

In contrast to above which the shape of imperfection distributes over entire surface of shells, localized area concepts with critical arc length also have been investigated considering elastic buckling behaviours with numerical analyses. In the design codes[2)3)] of shell bucklings, several curves for the actual buckling strength determined as the lower bound of the experimental results, are only applicable in cases where the actual initial geometry measured is within the tolerances in the shape and the maximum deviations of magnitude. Then a reduction factor to elastic classical buckling strength, called "knockdwon" factor, might be evaluated against shell's slenderness parameters[13]. Fortunately such buckling curves and design codes of shell bucklings are well-established and revising periodically by many researchers and others.

2.3 Previous studies in reticulated domes

For reticulated shells (single layer lattice domes) with perfect geometry as shown like in Fig.1(a), out of the displacement field obtained from elastic nonlinear buckling analysis or from elasto-plastic buckling analysis, most deformed portions (areas) are remarked. Here such localized portion can be related to a dimple with diameter of apparent buckling(or bending) wavelength. There a specific member among others may be stressed significantly. Also apparent buckling wavelength could be predicted preliminary in design stage by configuration shape parameters, like in Fig.1(b) and member properties, like in Fig.1(c) and (d), with support conditions.

The results[12)14)15)] obtained previously have shown that the reduction against linear buckling load, or equivalent shell's classical buckling load, is influenced by the configuration shape and constituent member properties[12)14)15)]. There a specific imperfection form and magnitude were adopted. The parameters have been considered are as follows. The member subtended half-angle as shown in Fig.1(b), $\theta_0 = \ell_0/2R$, which is representative of degree of curvature R and number of subdivision frequency n, and the member slenderness, $\lambda_0 = \ell_0/i_p$, are restricted[16)17)18)19)] to as $\theta_0 \geq 2degs.$ with n=4 to 6, and $60 \leq \lambda_0 \leq 150$, respectively. Namely, if the member length ℓ_0=3 and 4 meters, then the radius R and R/t_e using the equivalent thickness $t_e = 2\sqrt{3} \cdot i_p$ ranges from 40 to 60 meters and from 200 to 700, respectively. Also the dome span L ranges from 40 to 80 meters. Then more larger spanned reticulated shells will be planned, we have to investigate into the overall configuration shapes and dimensions, in conjunction with, the element size and sectional properties which are different from previous analytical models.

The imperfection form has been often assumed in previous studies as a single node (placed nearby boudary periphery) of inward type. The magnitude of imperfection has been given as the ratio to a characteristic rise height, $h \approx \ell_0 \cdot \theta_0$, of structural unit at apex or to an equivalent shell thickness t_e. Thus the magnitude always depends on both θ_0 and λ_0. The other considerations to the magnitude might come out relative to the overall span length L, radius of curvature R and total rise height H.

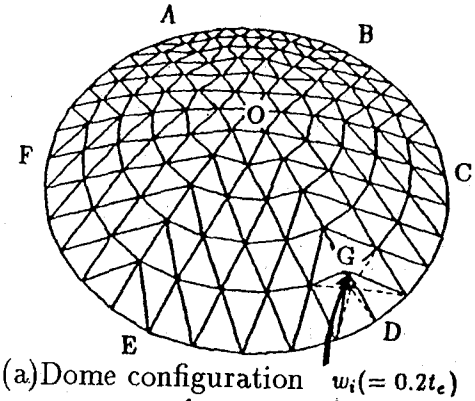

(a)Dome configuration $w_i(=0.2t_e)$

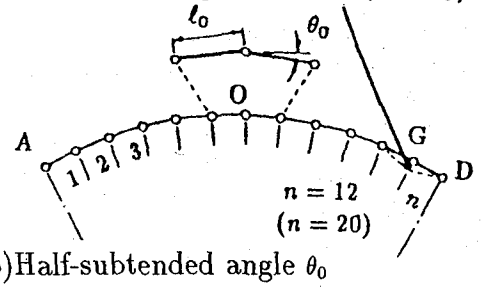

(b)Half-subtended angle θ_0

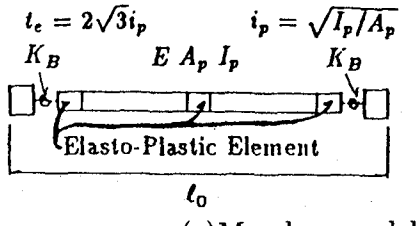

(c)Member model

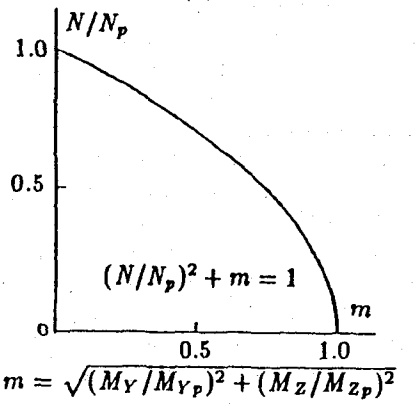

(d)Sectional strength interaction

Figure 1 Analytical model

3. Scope of Discussion

3.1 Analytical method

In order to estimate the buckling load reduction of large-spanned reticulated shell domes as shown in Fig.1(a) and (b), but having the number of subdivision frequency n=20 with the member length ℓ_0=10m, due to a specific initial shape imperfection and material plasticity, a discrete nonlinear model[21] which accounts the effect of nonlinear geometry (called, nonlinear elastic buckling analysis) and elasto-plastic behaviour (called, ealsto-plastic buckling analysis) is employed. Also the linear eigenvalue analysis for perfect structures is carried out. The effect of axial force on the member bending stiffness is considered with the slope-deflection method using stability functions[22][23] by extending three dimensional beam-column elements upon the theory of small finite deflection with bowing effect, since for analysis of reticulated shells where axial forces are large the geometric stiffness matrix approach requires that each member be broken up into more elements.

The constituent elements are modeled by nonlinear elastic beam-column members with elastic springs at connections, and three elasto-plastic spring systems, with zero-length plastic hinges, placed at both two external nodes and the center of member[14][17] just like the springs-in-series model[24], as shown in Fig.1(c). Also an approximate elastic plastic behaviour is used. The plastic effects are included by three elasto-plastic springs which are governed by the plastic flow rule based on the interaction of axial force and moment about the bending axes except torsions, as shown in Fig.1(d).

The ordinary structural matrix equations with condensed hybrid element in resultant single member can be formed with consideration of a total Lagrangian approach in view of the incremental formulations having tangent stiffness matrix. These equations are solved using the load and displacement control method with the linearized Newton-Raphson scheme[14][17]. It is assumed herein that buckling/collapse occurs whenever a limit point load or bifurcation load occurs.

3.2 Model parameters

Overall configurations of space frames play an important role of the structural behaviours. Likewise shells of double curvature, the imperfection sensitivity of spherically reticulated shells with rigid joints under uniform loading has been discussed in view of elastic nonlinear instability. In those studies[15][18] buckling load reduction to linear critical load would relate to characteristic buckling modes with buckling half wavelength. The overall buckling due to loss of member axial forces often arises from the combination of shape and member parameters. Also the flexural member buckling dominates when the member becomes more slender. On the other couplings of buckling failure modes in elasto-plastic collapse come out depending upon those parameters[14][15][18].

Table 1 Geometric shape parameters

θ_0(deg.)	R(m)	L(m)	H(m)	H/L
1.0	286.5	196.0	17.3	0.088
2.0	143.3	184.2	33.5	0.182

Table 2 Member properties

λ_0	$A_p(mm^2)$ ($\times 10^2$)	$I_p(mm^4)$ ($\times 10^5$)	$N_p(kN)$	$M_p(kNm)$
60	148.0	4100.0	3479.0	522.34
120	37.1	258.0	872.2	65.33

The parameters of analytical models are summarized in Tab.1 and Tab.2. Objective reticulated domes whose configuration with span L over 150 to 200 meters are depicted like in Fig.1(a)(b), are composed of straight circular tubes with rigid joints. And those are modeled having sectional strength interaction as shown in Fig.1(c)(d). Here the pipe member's properties are the yield strength, $\sigma_y = 235N/mm^2$ and the elastic modulus, $E = 206kN/mm^2$, respectively.

Such a large spanned dome with more shallower shapes will be constructed making the member subtended half-angle at apex less than $\theta_0 = 2degs.$ From previous studies into bucklings of reticulated domes, we adopt such analytical model parameters as in Tab.1 and Tab.2. These domes have the fundamental buckling behaviours as follows. When the case of $\theta_0 = 2degs.$ and $\lambda_0 = 120$, it seems to appear the member flexural buckling[9][12][16]. On the other, shell-like elastic bucklings[15][18][25] may be dominant in the case of $\theta_0 = 1deg.$ and $\lambda_0 = 60$. The characteristic interaction of shell-like buckling and member flexural buckling[15][18][25] may appear in the case of $\theta_0 = 1deg.$ and $\lambda_0 = 120$. The case of $\theta_0 = 2deg.$

Table 3 Fundamental buckling characteristics and buckling loads(kN)

θ_0 / λ_0	1deg. 60	2deg. 60	1deg. 120	2deg. 120
	shell-like elastic	shell-like plastic	coupled failure	non-shell member
ξ	16.05	8.02	8.02	4.01
$P^*_{cr,eq}$	260.0	1039.7	32.5	130.3
$N^*_{cr,eq}$	2483.3	4963.7	315.9	630.2
P^{lin}_{cr}	262.6	1012.3	31.6	92.0
$P^{el}_{cr,0}$	172.0	790.5	21.1	90.7
$P^{pl}_{cr,0}$	168.7	523.2	21.1	90.7

NOTE: $\xi = 12\sqrt{2}/\lambda_0\theta_0$=Shape Parameter

$\ell_{cr}/\ell_0 \approx 1.47\sqrt{\xi}$(Shell Analogy)

* $P_{cr,eq}$=Equivalent Classical Buckling Load per node.

* $N_{cr,eq} = P_{cr,eq}/6\theta_0$(Equivalent Axial Force).

$N_E(Euler's\ Force)$:

8350kN(λ_0=60); 519kN(λ_0=120)

and $\lambda_0 = 60$ seems to show the elasto-plastic shell-like buckling[17)18)]. Thus the analytical models with parameters summarized in Tabs.1 and 2 are representative to discuss the ultimate buckling capacities.

For the reticulated domes with perfect shapes, buckling analyses are separately carried out under each design reference loads P_0 per node, and the results are shown as in Tab.3. The design reference load P_0 is assessed in this study, by preliminary calculations using an equivalent shell theory under uniform vertical loading by multiplying tributary area $\sqrt{3}\ell_0^2/2$, and the Euler flexural buckling of members after the allowable member stress design of AIJ. Here the notations, P_{cr}^{lin}, P_{cr0}^{el} and P_{cr0}^{pl}, mean the buckling loads of linear eigenvalue analysis, non-linear elastic buckling analysis and elasto-plastic buckling analysis, respectively.

3.3 Imperfections for reticulated domes

(1) Specifying the imperfection

Insofar as an elastic equivalent to continuum shells may hold, the length spanned by local imperfections, often called the gauge length or template length in design codes of shells, is specified by the notation[6)7)], of $\ell_{cr} = 3.5\sqrt{Rt_e}$. Here R is the radius of curverture related to the shape parameter of reticulated dome as $R = \ell_0/\sin\theta_0$, and $t_e = 2\sqrt{3}i_0$ is the shell thickness calculated by using the radius of gyration, i_p, of member. Also sometimes the rise of structural unit at apex in reticulated dome, h, which coincides with $h = \ell_0 \sin\theta_0$, is used to specify the imperfection magnitude, $\epsilon_0 = \delta_0/h$, in case of snap-through bucklings of space trusses.

The maximum radius of curvature, R_{imp}, for equivalent spherical shell as a local imperfection measure is also adopted, then using relation below[6)], the critical ratio of R_{imp}/R goes to over two.

$$\frac{\delta_0}{t} = \frac{\ell_{cr}^2}{8} \times (1 - \frac{R}{R_{imp}}) \times \frac{1}{Rt} \qquad (1)$$

where the increased-radius imperfection can relate to the inward dimple imperfection as the shape function assumed in Błachut and Galletly[6)], as below with the notation of δ_0 replaced by w_0 for maximum depth, in this paper.

$$w(S) = w_0 \times \{1 - [\frac{S}{S_{imp}}]^2\}^3 \qquad (2)$$

Here $S_{imp} = \ell_{cr}/2$, and S means the distance measured from center of the meridional extent of the imperfection with the maximum depth of w_0, assigned its length to nodes within circle of ℓ_{cr} in diameter. Meanwhile the maximum tolerance of overall imperfection often is related to R and the ratios are from $1/100$ to $1/200$, or about $R/3000$ after Dulácska[20)]. Another method of specifying construction deviations in framed buildings is often based on the ratio of imperfection amplitude w_0 to the length of longest member which means the maximum slenderness ratio of member in structures (e.g. Morris[9)]).

(2) Employed imperfections

This study considers the shape of imperfection and the magnitude, which are summarized in Tabs.4,5 and 6 as followings:

a)each of single nodes on a half of meridian along D to O, as shown in Fig.2, which corresponds to the case of $\ell_{cr} = 2\ell_0$ with w_0=100mm, is used to compare the results with previous studies[14)15)] which corresponds to the case of Type A,

b)the smooth dimple in shape defined as Eq.(2) which is in a circular area spanned over several nodes with the diameter, ℓ_{cr}, measured from the boundary, as shown in Fig.2 with solid lines like Type B, is adopted first,

c)the maximum magnitude at the node placed at center of dimple circle, w_0, is determined by a fraction of member length as $w_0 = k \times \ell_0$ with $k = 0.01, 0.02$,

d)the smooth dimple also located on the apex of dome, just axisymmetric imperfection mode with variable diameter, ℓ_{cr}, as shown in Fig.2 with broken lines, Type C, is used.

Here each ℓ_{cr} as shown in Tab.4 does not equal to m$\times\ell_0$, m=the number of members. Then for Type B and Type C as shown in Fig.2 amplitudes of nodal imperfections are assumed as ℓ_{cr}=m$\times\ell_0$ and assigned by using Eqn(2).

The ratio of imperfection magnitude to the reference length may be convertible each other as summarized in Tab.5 (for $\epsilon_0 = w_0/t_e$) and Tab.6 (for $\epsilon_g = w_0/t_e$), respectively.

In contrast, Ueki et al.[19)] reported the maximum imperfection amplitude of about 3(mm) from observation in vertically downwards of realsized model having member length of 3(m). Despite configuration shape parameters, it seems that space frames could be constructed with rather accuray in actual situations. The imperfections assumed with the maximum amplitudes, w_0, are given to nodes vertically downwards in this study.

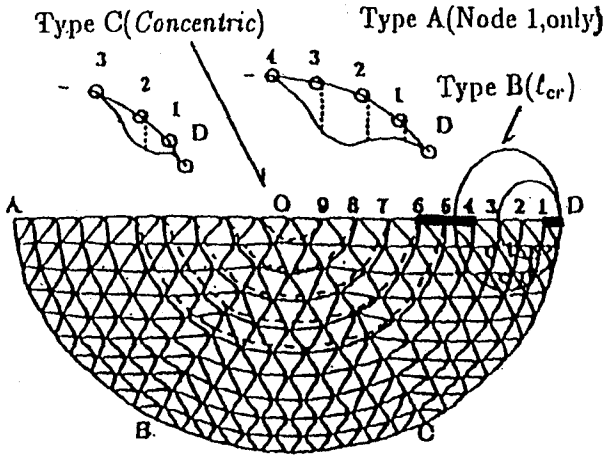

Bold lines::Critical members(N_{max})

Broken lines::Concentric circles

(m=Number of members)

Figure 2 Geometric imperfection shapes

Table 4 $\ell_{cr} = 3.5\sqrt{Rt_e}$(meters)

θ_0	$\lambda_0 = 60$	$\lambda_0 = 120$
1deg.	45	32
2deg.	32	23

Table 5 $\epsilon_0 = w_0/h$

θ_0	1deg.	2deg.
$w_0 = 50mm$	0.29	0.14
$w_0 = 100mm$	0.57	0.28

Table 6 $\epsilon_g = w_g/t_e$

λ_0	60	120
$w_0 = 50mm$	0.08	0.17
$w_0 = 100mm$	0.17	0.35

4. Numerical Results

Ordinary imperfection sensitivity analyses for continuum shell bucklings have been investigated theoretically or experimentally in view of a family of Koiter's approach[2)3)10)]. Then a "knockdown" factor as the ratio of the actual buckling load/stress to the theoretical (classical) critical load/stress has been evaluated against the magnitude of the deviation from the exact/ideal configuration shape. However for reticulated shells require many more variables in their description for formula with relating critical load/stress reduction to imperfection magnitude parameters.

In order to evaluate a "knockdown" factor of reticulated domes, we have some calculations of which the definitions of characteristic "knockdown" factors as the reduction of buckling loads in this study, are given as follows. For the elastic and elasto-plastic knockdown factors, ρ and ρ_{pl}, mean the ratio of P_{cr}^{el} and P_{cr}^{pl} to P_{cr}^{lin}, respectively. For the reduction from buckling for perfect geometry to for imperfect cases, ρ' and ρ'_{pl} mean the ratio of buckling loads to P_{cr0}^{el} and P_{cr0}^{pl}, respectively.

For the perfect domes of analytical model with combinations of θ_0; λ_0, fundamental elastic buckling behaviours are governed mainly by θ_0. Representative mode or displacement field along a half of meridian D to O, as shown in Fig.2, appears in a specific manner. When θ_0=1deg., then the most deformed portion locates near boundary periphery including nodes 1 and 2 with shorter wavelength. On the other, in case of θ_0=2degs., longer wavelength spanned from nodes 3 to 6 appears with lesser edge effects. The most stressed members also locate within such deformed portions; (1)for θ_0=1deg. with λ_0=60 and 120, members D-1 and 1-2 on meridonal lines, repectively, and (2)for θ_0=2degs. with λ_0=60 and 120, members 4-5 and 5-6, repectively. At the elasto-plastic buckling load, the members having maximum axial forces just move more towards the apex but adjoining to the most stressed members at elastic bucklings.

4.1 Single node imperfection (Type A)

The elastic and elasto-plastic buckling reductions are given in Fig.3 and Fig.4 for ρ and ρ' against w_0=100mm, respectively. In case of θ_0=1deg. and λ_0=60, the reduction appears significantly in lower value at the node position 2. On the other hand, the reduction for case of θ_0=1deg. and λ_0=120 seems to be independent on the node position at least in elastic bucklings.

From the comparison of the results from Ueki et al.[14)] and Mutoh et al.[15)], which were obtained in case of imperfection magnitude, $w_0 = 0.2t_e$, despite of $\ell_{cr} = 2\ell_0$ with direction in center of curverture at

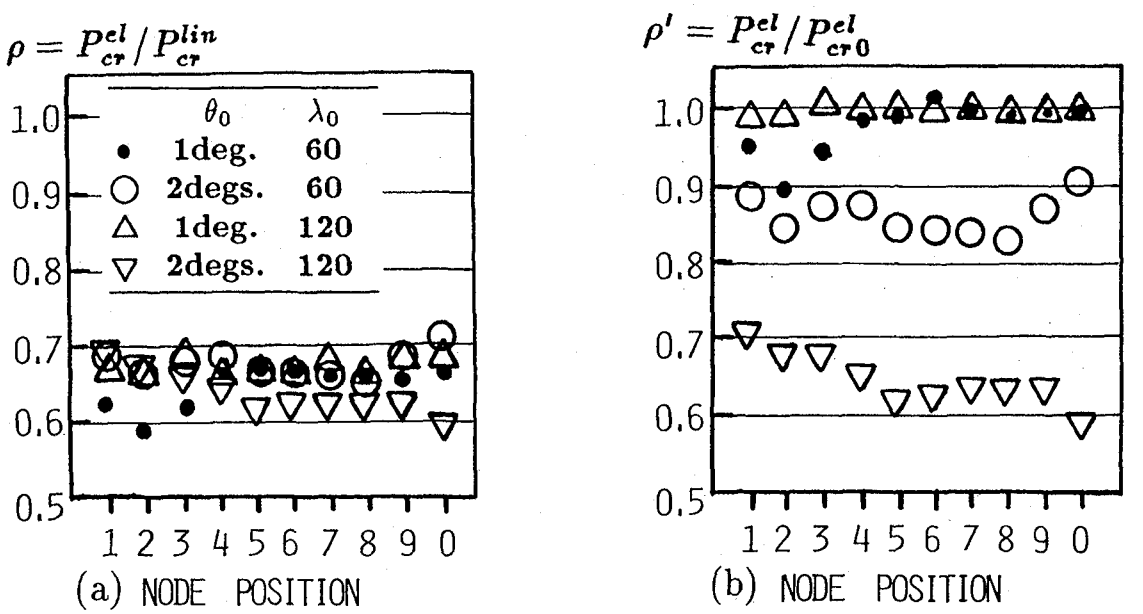

($w_0 = 100mm$ for Single Node along Meridian)

Figure 3 Elastic buckling reduction

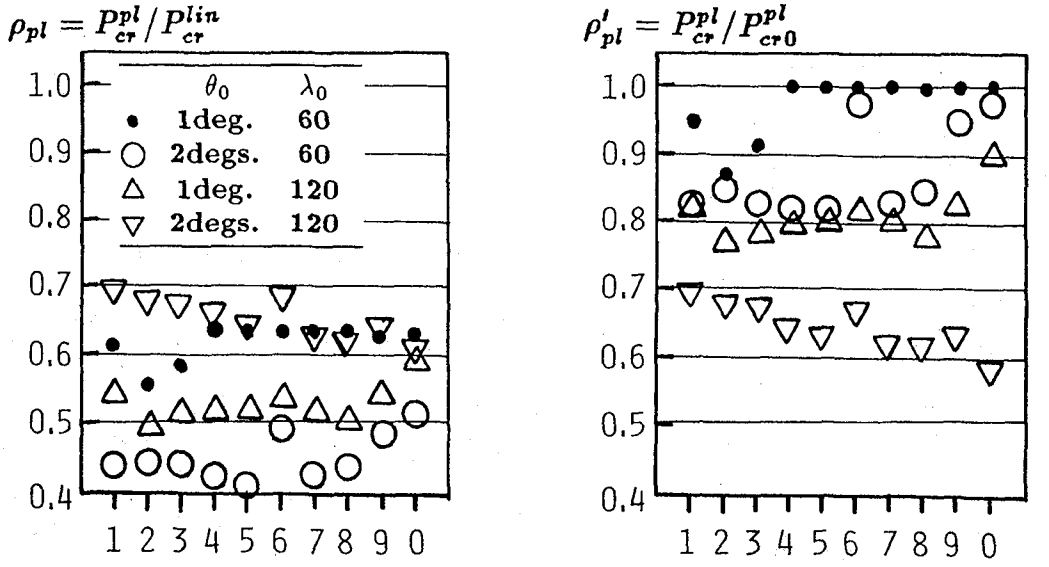

($w_0 = 100mm$ for Single Node along Meridian)

Figure 4 Elasto-plastic reduction

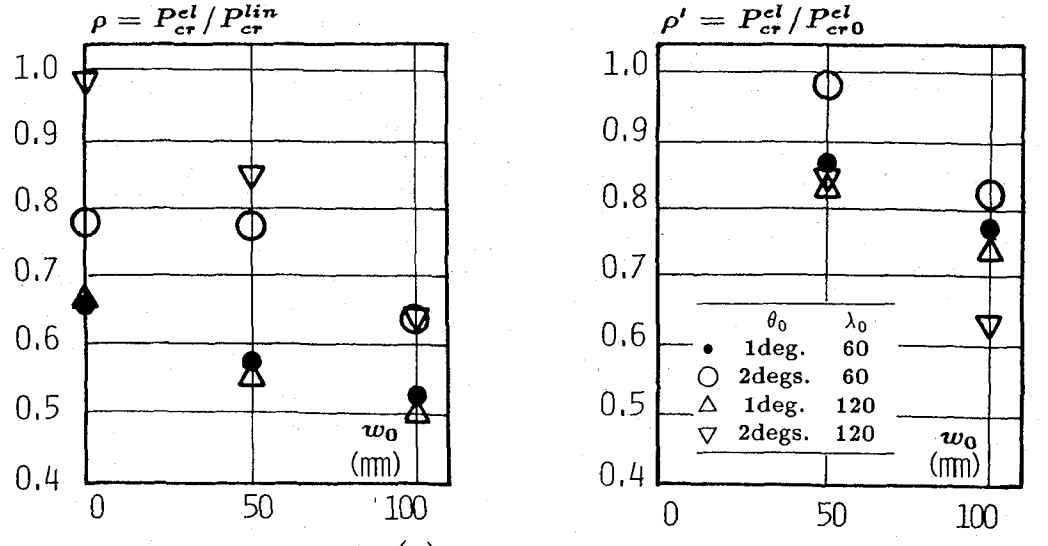

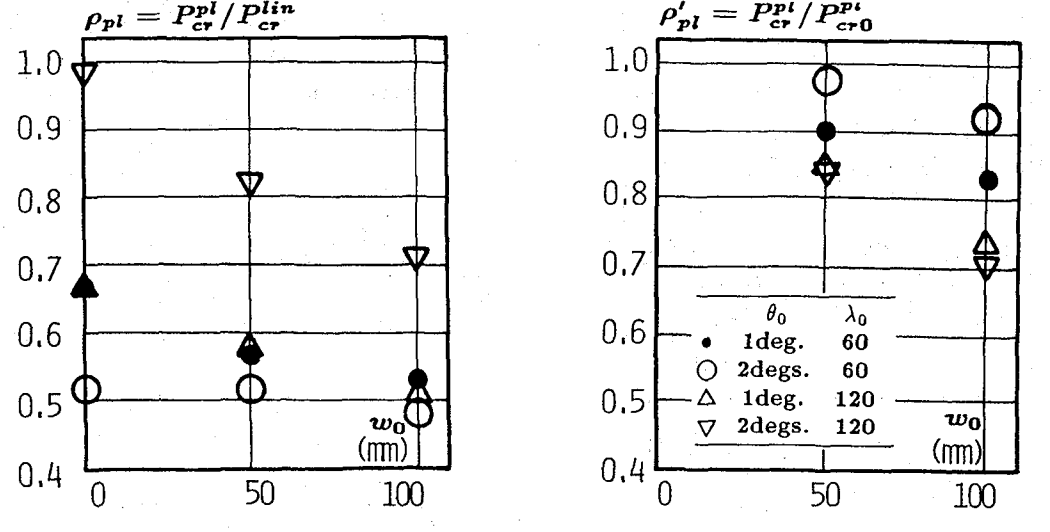

Figure 5 Imperfection sensitivity for w_0=50, 100mm

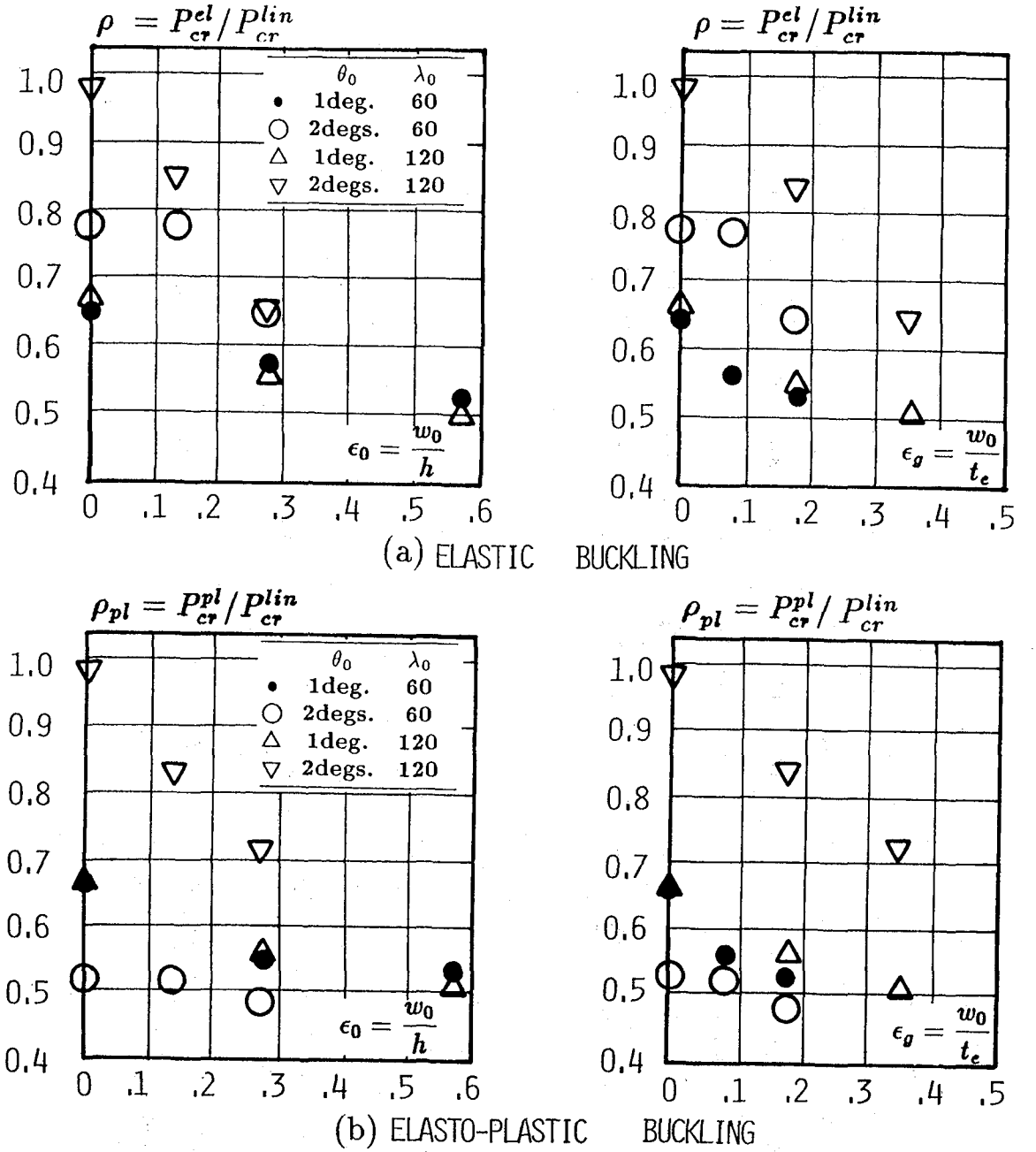

Figure 6 Knockdown factor curve against ϵ_0; ϵ_g

the node position 1, the reductions almostly coincide each other, except for the cases of (θ_0=2degs. , λ_0=60) and (θ_0=2degs., λ_0=120). Furthermore, the node position affecting reductions tends to be more internal in a dome.

4.2 Smooth dimple (Type B)

The comparisons of imperfection sensitivities with magnitudes, w_0=50,100mm, are given in Fig.5. When the cases of θ_0=1deg. and (θ_0=2degs. , λ_0=60) are remarked, those sensitivities are not so pronounced. The other case, θ_0=2degs. and λ_0=120, more significant reduction ρ'; ρ'_{pl} from loads for perfect shapes is observed.

In ordinary manner, characteristic "knockdown" factors can be depicted as in Fig.6, against ϵ_0 and ϵ_g which are illustrated in Tab.5 and Tab.6. From this figure the cusp-like curve is obtained for the case of θ_0=1deg. and λ_0=60 and 120, which is resembled with the results from Koiter's approach for ocntinuum shells. In the elastic buckling reductions, Fig.6(a), when the results of the case, θ_0=1deg., show the lower bounds. But the case of θ_0=2degs. and λ_0=60, shows significant reductions in the elasto-plastic bucklings even to 0.4 for w_0=100mm but ϵ_g= 0.17, as in Fig.6(b), but for perfect shape ρ_{pl} shows a half of linear buckling load P_{cr}^{lin}.

4.3 Smooth dimple (Type C)

First of all, the influence of imposed imperfection area just relapced ℓ_{cr} to m×ℓ_0 having center of concentric O, where m means number of members along meridian with center O, as shown in Fig.2 is compared. From Fig.7(a) and (c) for case of $\theta_0 = 1deg$, the reduc-

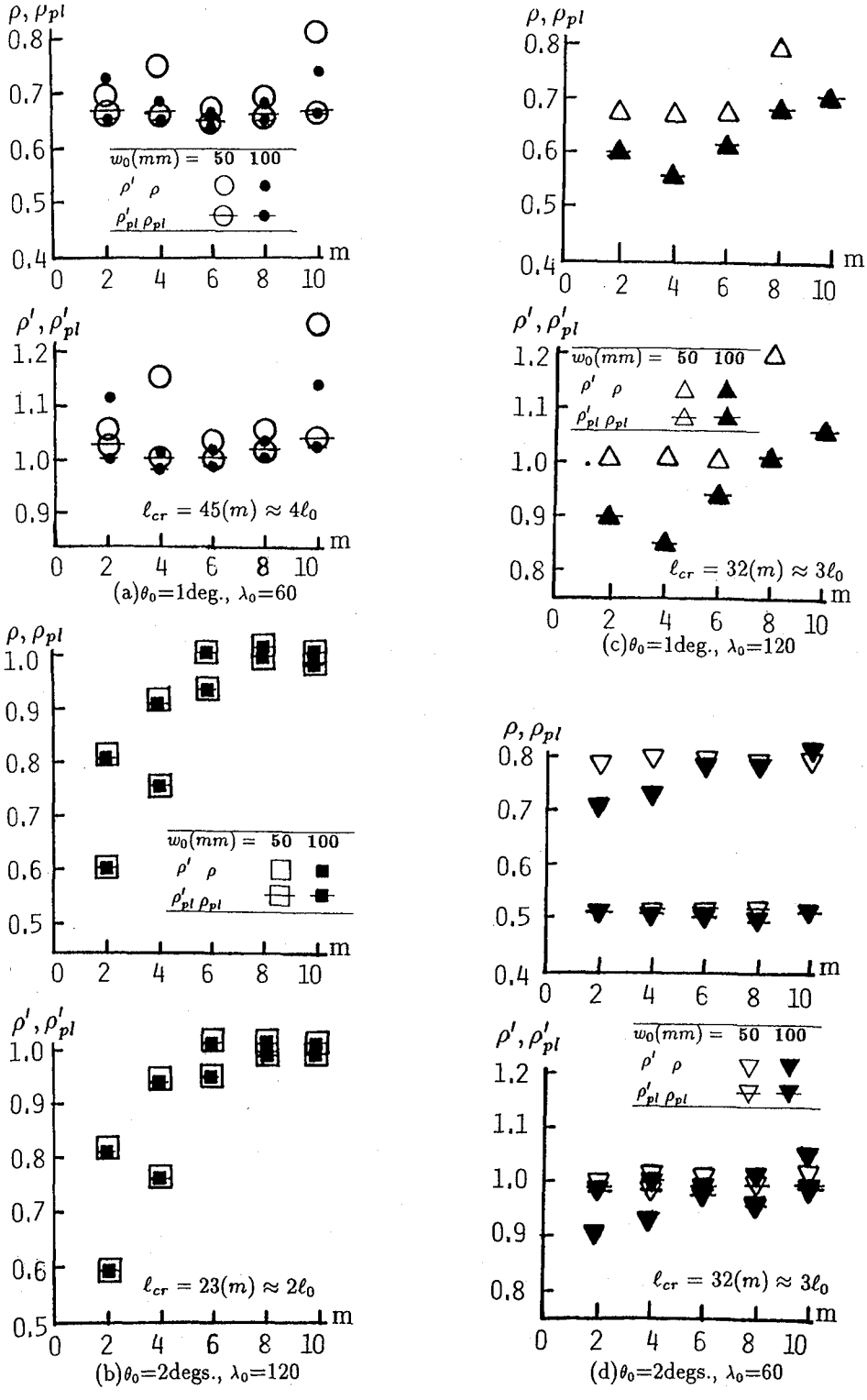

Figure 7 Buckling reduction versus imperfection area spanned by m×ℓ_0 at apex

tions appears in characteristic manner in contrast to the case of θ_0=2degs. In Fig.7(c) each marks of empty and blacked triangles for ρ, ρ_{pl} and ρ', ρ'_{pl} coincide with each other. Also in Fig.7(b) similar coincidence is remarked just below m=6, when ℓ_{cr}=60m.

However the results for λ_0=60 show the pronounced reduction in the range of m between 6 and 8 which nearly corresponds to 1.5 or 2 times ℓ_{cr}=45(m). On the other hand the reduction for case of λ_0=120 may be affected within m×$\ell_0 \leq$ 60(m) which ranges about 2 times ℓ_{cr}=32(m).

As before-mentiond fundamental buckling behaviours of analytical models, nodes located on central portions always do not so be deformed relative to more outer prtions near boundary, effects of shape imperfections of concentric dimples Type C on characteristic load reductions are not no significant. In case of θ_0=2degs. which often shows fundamentally the member flexural buckling, the effect of dimple diameter m ×ℓ_0 is remakable from Fig.7(b). However ℓ_{cr} for

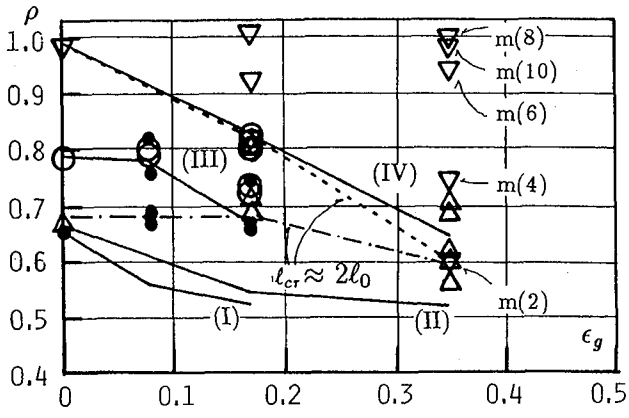

(a) Elastic buckling reduction

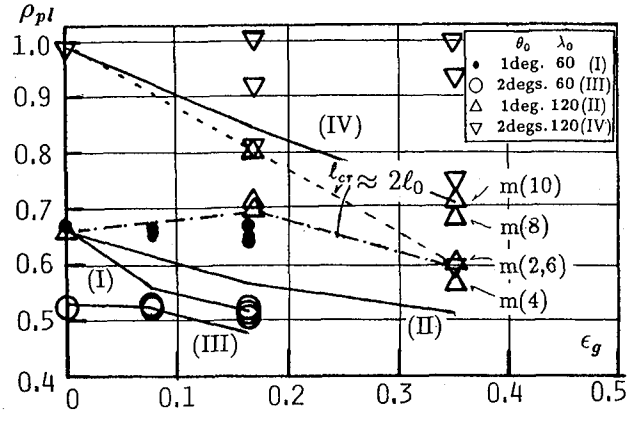

(b) Elasto-plastic reduction
(I)(II)(III)(IV):Type B

Figure 8 Knockdown factors against ϵ_g(Type C)

each combination of θ_0; λ_0 may affect the load reductions except the case of θ_0=2degs. with λ_0=60. Also despite Type C imperfections most deformed portions almost always appear in nodes placed outer area on dome surface.

Next, in order to disucuss the imperfection sensitivity in case of smooth dimple at apex (Type C), all the plots for ρ and ρ_{pl} given in Fig.8, which are adopted from Fig.7, lead to be higher than the plots shown in Fig.6, against $\epsilon_g \geq 0.17$, except the case of θ_0=2degs. with λ_0=120 as denoted by *triangledown* marks. From these comparisons the influence of the maximum imperfection magnitude and the location introduced on the buckling load reductions have to be considered when designers face to select a reticulated dome configuration. However the attention might be payed to local imperfection distribution spanned over approximately $2\times\ell_0$ to $4\times\ell_0$ in smooth dimple shape of Type B, introduced into periphery in a dome.

5. Strength Evaluation

In shell-like buckling of reticulated shells, one may often adopt the reduction curve described in the design codes, but calibrated against the special shell's slenderness $\Lambda_s = \sqrt{\sigma_y/\alpha\sigma_{cl}}$. Here σ_{cl} means the classical bifurcation buckling stress and α is a characteristic "knockdown" factor for continuum shells derived empirically from many experimental studies. One of buckling design formula for continuum shells is the type of Schwarz-Rankine formula(e.g. DIN[4], ECCS[5]) or the modified Dunkerley formula[10] given below, respectively.

$$\frac{\sigma_u}{\alpha\sigma_{cl}} + (\frac{\sigma_u}{\sigma_y})^2 = 1 \qquad (3)$$

$$\frac{\sigma_u}{\sigma_y} = \frac{1}{\sqrt{a\Lambda_s^4 + b\Lambda_s^2 + 1}} \equiv \chi(\Lambda_s) \qquad (4)$$

Also the ultimate load capacity of continuum shells has been given semi-empirically[13] by the plasticity reduction factor ζ multiplied with $\alpha \times \sigma_{cl}$, where ζ equals to $\Lambda_s^2 \cdot \sqrt{\Lambda_s^2/4 + 1} - \Lambda_s^4/2$.

5.1 Buckling curves

For reticulated shells, the generalized slenderness very similar to the above slenderness without reduction factor like α could be determined as $\Lambda = \sqrt{N_y/N_{cr}^{lin}}$ or $= \sqrt{\sigma_y/\sigma_{cr}^{lin}}$ for perfect configurations through a linear eigenvalue analysis applied to the whole structure[16][17][18]. Here N_y=the yield axial force, N_{cr}^{lin}=the critical axial force of a specific element within a characteristic buckling area over structure, just corresponding to the linear buckling load P_{cr}^{lin}. We have presented several buckling curves[16][17][18] on the basis of above Eqns(3) and (4) as well as of equivalent column flexural buckling formula.

We introduced the assumption of linear dependence between applied loading and internal maximum axial force in a specific element even to the ultimate state. Becuase it is hard to compute the ultimate buckling capacity of reticulated shells having huge number of elements at design stage, but one can, in practical, carry out the linear eigenvalue analysis as well as linear elastic stress analysis on computers. In order to estimate the buckling capacity by only carrying out eigenvalue analysis, following assumption is made. Using the reference design load P_0 and the axial force N_0 obtained from linear elastic stress analysis, the estimation of ultimate buckling strength N_u and ultimate capacity P_u is given as below:

$$N_u = P_u \times \frac{N_0}{P_0} \; ; \; P_u = N_u \times \frac{P_0}{N_0} \qquad (5)$$

The effectiveness of the assumption about the load carrying capacity prediction should be discussed. But in this paper this issue is just beyond scope, and some investigations will appear in the near future[27].

5.2 Comparisons with design curves

In order to evaluate the capacity reduction for reticulated shells, comparisons in-between the buckling curves are made. Insofar as a single design curve may be prefered, a "knockdown" factor α=0.5 but replaced from σ_{cl} to $\sigma_{cr}^{lin} = N_{cr}^{lin}/A_p$ in Eqn(3), from those previous studies[15][23] might be appropriate and from the results presented in this paper. Or another value, say, α=0.8, may be applied to the modification of strength

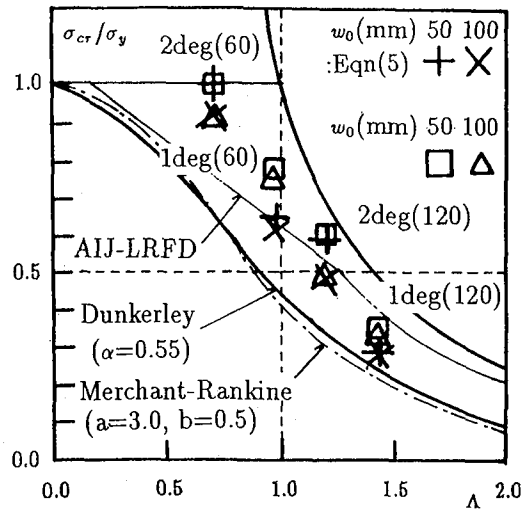

Figure 9 σ_u/σ_y and Λ curves (Type A)

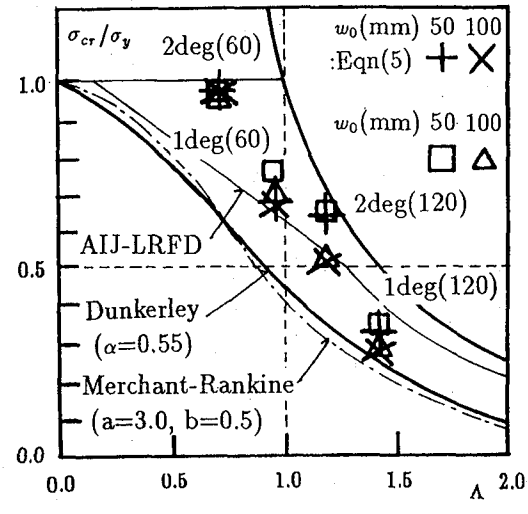

Figure 10(a) σ_u/σ_y and Λ curves (Type C;m=2)

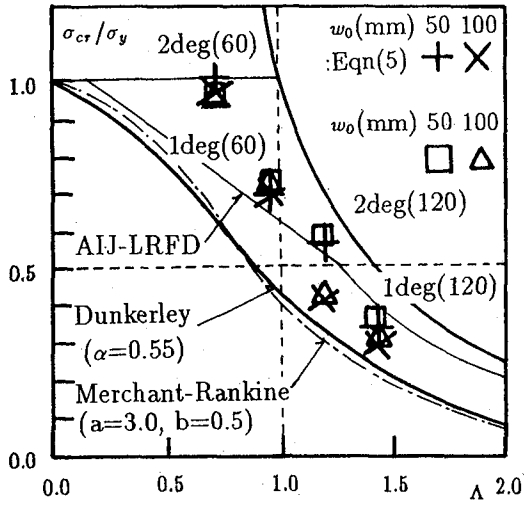

Figure 10(b) σ_u/σ_y and Λ curves (Type C;m=4)

curves if some kind of classification due to fundamental structural behaviour is needed.

First, we illustrate the strength curves by using results obtained from aforementioned imperfection sensitivity analyses as a function of Λ. Here each Λ for θ_0=1deg. and λ_0=60, 120 is 0.995 and 1.446, respectively. Also for θ_0=2degs. each Λ is 0.723 and 1.200 for λ_0=60 and 120, respectively. In Figs.9, 10 and 11 of which results correspond to previously specified imperfections, Type A, Type C and Type B, respectively. In case of Type C, those plotts were given only for most reduced values obtained from numerical analysis with variable $\ell_{cr} = m \times \ell_0$, to each configuration models. Namely, the coefficient m stands for 2 and 4. In case of Type B, m also given corresponds to each the coefficients approximately deduced from Tab.4 against the member length ℓ_0. Among those it is observed in the range below Λ=1.0 that the imperfection like Type B may affect the reduction of buckling strength rather than other cases.

Since one can replace the slenderness Λ to Λ_s, like the shell's slenderness including a "knockdown" factor, the buckling curve for reticulated domes with localized geometric imperfections as a function of Λ and Λ_s are feasible as shown in Figs.11,12 and 13 with Type B geometric imperfections, respectively. In these figures, the results from not only estimations by Eqn(5), denoted by marks + with dotted lines, but also N_{max} obtained directly for the critical member with marks □, ○, △ and ×, are depicted in parallel against slenderness Λ and Λ_s, respectively. All the marks show the reductions of maximum axial stress ratio, which correspond to be denoted as upper and lower posions due to w_0=50 and 100mm, respectively.

In Fig.11 plots of normalized buckling strength as a function of Λ are compared with not only column flexural buckling curves, denoted as AIJ-LRFD and AIJ-Allowable, but also uniform reductions in elastic buckling strength given by $0.8/\Lambda^2$ and $0.5/\Lambda^2$. On Figs.12 and 13, including shell design curves, the buckling strength as a function of Λ_s with α=0.5 and 0.8 is shown, respectively. Firstly, the estimated results from Eqn(5) are almost always lower than the values directly obtained. Furthermore the coincidende between the plots and the ECCS design curve with α=0.8 in the range of slenderness Λ_s by 1.0 is remarkable. Secondary, from Fig.11, the strength curves for column flexural buckling seems not to be appropriate, in particular for Λ by 1.0. On the other, both results for normalized strength are just inbetween the curves $0.8/\Lambda^2$ and $0.5/\Lambda^2$.

Of cource an idea of classified buckling curves like multi-column strength curves will be available, since the reduction factor depends on the shape parameters θ_0 and λ_0 or the charateristic buckling wavelength. However we may adopt the comment on one of engineering judgment for a "knockdown" factor stated by Hoff[2]: insofar as the imperfection sensitive sturcutre may be concerned, the upper bound of reduction factor might be restricted by 0.5 considering even uncertainty of nature of geometric imperfections at design stages.

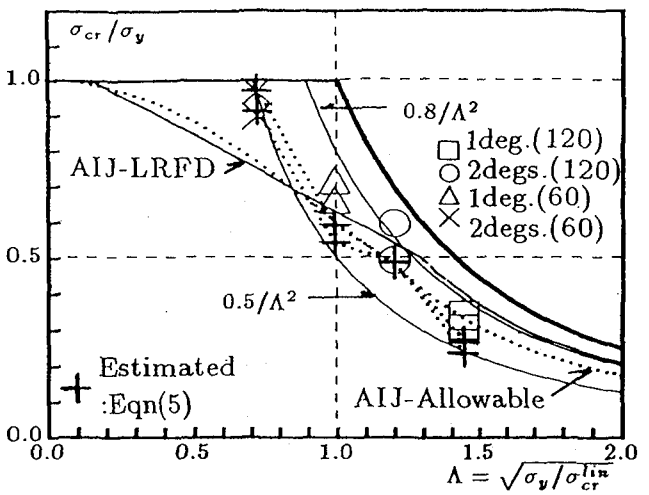

Figure 11 σ_u/σ_y and Λ curves(Type B)

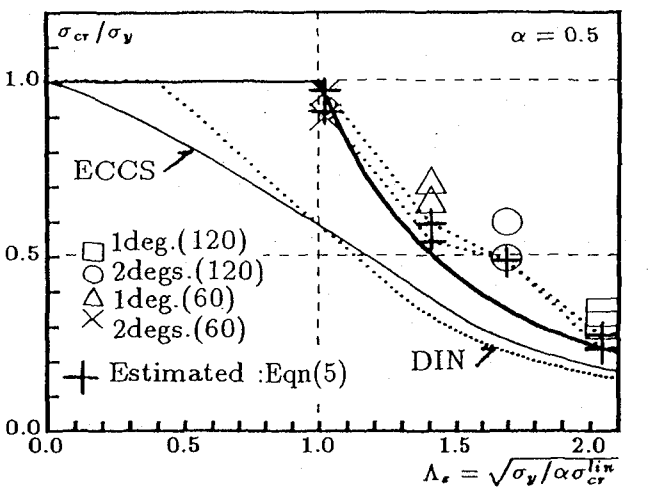

Figure 12 Buckling strength curve against Λ_s(Type B)

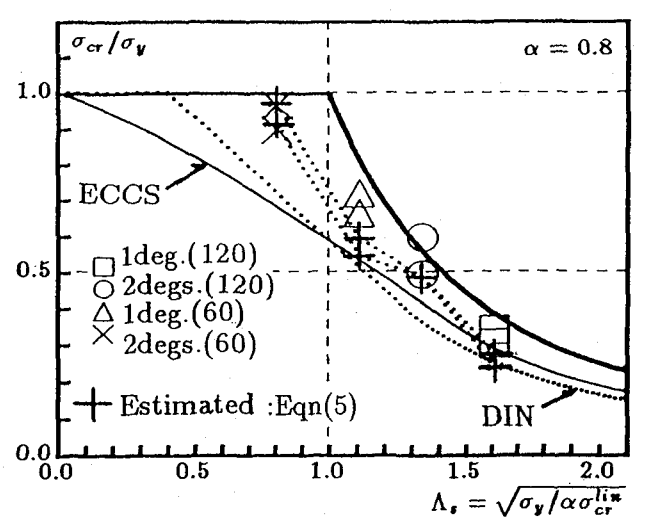

Figure 13 Buckling strength curve against Λ_s(Type B)

6. Conclusions

From above-mentioned results, when inward smooth dimple shape imperfections with characteristic magnitudes relative to the constituent member length in reticulated domes with rigid joints is applied to evaluate the buckling load reduction, followings are found. (1)The elastic and elasto-plastic buckling reductions appear not so pronounced with comparison of those for continuum shells. (2)Amongst buckling load reductions the case of dimple axisymmetrically located on the apex shows relative lower than the case located on near the dome boundary.

However the buckling load reductions of domes with elastic shell-like buckling characteristics has to be investigated further in view of comparison with elasto-plastic bucklings of spherical shells. This paper discussed the buckling strength curves for reticulated shells with locally distributed geometric imperfections in view of characteristic slenderness. The results lead to a potential evaluation method for buckling capacity of space frames in a similar way of ordinary practical design procedure of columns in a frame building and of continuum shells.

References

1)IASS Wroking Group on Spatial Steel Structures (Nr.8)(1984). *Analysis, Design and Realization of Space Frames* (a State-of-the-Art Report), IASS Bulletin, No.84/85(Special Issue), Madrid.

2)Hoff, N.J.(1969). Some Recent Studies of the Buckling of Thin Shells. *The Aero. J. of R. Aero. Soc.* 73(December), pp.1057-1070.

3)Fung, Y.C. and Sechler, E.E.(1974). *Thin - Shell Structures Theory, Experiment and Design*, Prentice-Hall, New Jersey.

4)DIN 18 800 Part4(1993). *Structural Steelwork: Analysis of Safety against Buckling of Shells*, Beuth Verlag GmbH, Köln.

5)ECCS(1983). *The Buckling of Shells.* In European recommendations for steel construction, Brussels, Publication 29.

6)Błachut,J. and Galletly,G.D.(1990). Buckling Strength of Imperfect Spherical Caps - Some Remarks, *AIAA J.* Vol.28, No.7, p.1317-1319.

7)Galletly,G.D. and Błachut,J.(1991). Buckling Design of Imperfect Welded Hemispherical Shells subjected to External Pressure. *Proc. of Instn. Mech. Engrs.* Vol.205, pp.175-188.

8)Jullien, J.F.(1991). *Buckling of Shell Structures, On Land, In the Sea and In the Air*, Elsevier Applied Science, London.

9)Morris, N.F.(1991). Effect of Imperfections on Lattice Shells, *J. of Structural Engineering* Vol.117, No.6, ASCE, p.1796-1814.

10)Kollár, L. and Dulaćska, E.(1984). *Buckling of Shells for Engineers*, John Wiley & Sons.

11) Borri, C. and Spinelli, P.(1988). Buckling and Post-Buckling Behaviour of Single Layer Reticulated Shells affected by Random Imperfections, *Compute and Structures*, Vol.30, No.4, p.937-953.

12) Suzuki,T., Ogawa, T. and Tanaka, M.(1989). Elastic Buckling Loads of Rigidly Jointed Single Layer Reticulated Domes with Initial Imperfection. *Proc. of Congress of Madrid - 30 Anniversary of IASS - 10 Years of Progress in Shell and Spatial Structures*, Vol.4.

13) Samuelson, L.Å. and Eggwert, S.(1992). *Shell Stability Handbook*, Elsevier Applied Science, London.

14) Ueki, T., Kato, S., Kubodera, I. and Mukaiyama, Y.(1991). Study on the Elastic and Elasto-Plastic Buckling Behaviour of Single Layered Domes composed of Members having Axial and Bending Springs at Both Ends. *Proc. of Symp. of Copenhagen - Spatial Structures at the Turn of the Millenium - Copenhagen*, Denmark, Vol.3, p.93-100.

15) Mutoh, I., Ueki, T. and Kato, S.(1992). On Estimation of the Buckling Load of Lattice Domes by Generalized Slenderness. *IASS - CSCE International Congress 1992 - Innovative Large Span Structures - Toronto*, Canada, Vol.2, p.564-575.

16) Kato, S., Yamada, S., Takashima, H. and Shibata, R.(1991). Study on the Buckling Stress of a Rigidly Jointed Single Layer Reticular Dome. *J. of Struct. Constr. Engng.* No.428, AIJ. pp.97-105 (in Japanese).

17) Kato, S., Shomura, M., Shibata, R. and Ueki, T.(1992). Estimation of Elasto-Plastic Buckling Loads for Reticular Domes on a Circular Plan, *J. of Struct. Constr. Engng.* No.439, AIJ. pp.111-119 (in Japanese).

18) Shibata, R., Kato, S. and Ueki, T.(1993). Study on an Elasto-Plastic Buckling Load of a Rigidly Jointed Single Layer Shallow Reticular Dome. *J. of Struct., Constr. Engng.* No.449, AIJ. pp.143-153 (in Japanese).

19) Ueki, T., Mukaiyama, Y., Shomura, M. and Kato, S.(1991). Loading Test and Elasto-Plastic Buckling Analysis of a Single Layer Latticed Dome. *J. of Struct. Constr. Engng.* No.421, AIJ. pp.117-128 (in Japanese).

20) Dulácska, E.(1981). Explanation of the Chapter on Stability of the Recommendations for Reinforced Concrete Shells and Folded Plates and a Proposal to its Improvement. *IASS Bulletin*. No.77, p.3-18.

21) Kusama, H., Shibata, R. and Kato, S.(1992). Ultimate Strength Analysis of Steel Pipe Arches by Nonlinear Buckling-Slope-Deflection Elements. *J. of Struc. Engng*, Vol.38A, pp.189-202, March.,1992(in Japanese).

22) Livesley, R. K.(1964). *Matrix Method of Structural Analysis*, Pergamon Press, London.

23) Chen, W.F. and Lui, E.M.(1987). *Structural Stability*, Elsevier Science Publishing Co., Inc.

24) Chen, W.F. and Chan, S.L.(1995). Second-Order Inelastic Analysis of Steel Frames using Element with Midspan and End Springs. *J. of Structural Engineering* Vol.121, No.3, p.530-541.

25) Mutoh, I. and Kato, S.(1993). On Relationships between Ultimate Strength of Single Layer Lattice Dome and Buckling Curves of Spherical Shell. *J. of Stuct. Constr. Engng.* No.449, AIJ. pp.155-161(in Japanese).

26)AIJ(1986). *Recommendation for Quality Criteria and Inspection Standards of Steel Structures*, Architectural Institute of Japan (in Japanese).

27) Kato, S. and Mutoh, I.(1995). Evaluation of Collapse of Reticulated Shells by Equivalent Column Slenderness. *Proc. Int. Conf. on Structural Stability and Design*. Sydney (to present).

(Received September 18, 1995)